Carbohydrate Polymers 105 (2014) 26–33

Contents lists available at ScienceDirect

Carbohydrate Polymers

journal homepage: www.elsevier.com/locate/carbpol

Isolation, characterization and antioxidant activity of polysaccharide from *Schisandra sphenanthera*

Ting Zhao[a], Guanghua Mao[b], Weiwei Feng[b], Riwen Mao[c], Xiaoyun Gu[a], Ting Li[a], Qian Li[d], Yongtuan Bao[a], Liuqing Yang[a,*], Xiangyang Wu[e,**]

[a] School of Chemistry and Chemical Engineering, Jiangsu University, Xuefu Rd. 301, Zhenjiang 212013, China
[b] School of Food and Biological Engineering, Jiangsu University, Xuefu Rd. 301, Zhenjiang 212013, Jiangsu, China
[c] Nucell Biotechnology Co. Ltd., Jingsi Rd. 2, Zhenjiang 212009, Jiangsu, China
[d] School of Pharmacy, Jiangsu University, Xuefu Rd. 301, Zhenjiang 212013, Jiangsu, China
[e] School of the Environment, Jiangsu University, Xuefu Rd. 301, Zhenjiang 212013, Jiangsu, China

ARTICLE INFO

Article history:
Received 10 December 2013
Received in revised form 7 January 2014
Accepted 16 January 2014
Available online 28 January 2014

Keywords:
Schisandra sphenanthera Rehd. et Wits.
Polysaccharide
Structural elucidation
Methylation analysis
NMR spectroscopy
Antioxidant activity

ABSTRACT

A water-soluble polysaccharide (SSPP11) from *Schisandra sphenanthera* was purified by DEAE-cellulose and Sephadex G-100 columns. Structure of SSPP11 and its antioxidant activity was evaluated. Results showed that SSPP11 has a molecular weight of 5.3×10^3 Da and is composed of Man, Glu and Gal. A linkage analysis and NMR study revealed that SSPP11 has a backbone of →1)-D-Man-(6→, →1)-D-Man*p*-(2→, →1)-D-Glu*p*(4→, →1)-D-Glu*p*-(6→, →1)-D-Gal*p*-(4→, →1)-D-Gal*p*-(4,6→ and →1)-D-Man*p*-(3,6→, with Man, Glu and Gal, which are distributed in branched chains. The Congo red absorption test revealed that SSPP11 has a triple helix stereo-configuration. Moreover, antioxidant activity of SSPP11 was stronger than the polysaccharide from *Schisandra chinensis* (Turcz.) Baill. In sum, this study demonstrates that a moderate molecular weight, triple helix stereo-configuration and higher degree of branching are beneficial for exerting antioxidant activity.

1. Introduction

Polysaccharide, a type of macromolecule polymer, is commonly found in plants, animals and microorganisms (Mao et al., 2014; Wang et al., 2013; Wu et al., 2012; Zhao et al., 2013; Zhu et al., 2014). A previous study indicated that polysaccharides not only play an important role in the growth and development of living organisms (Lin, Zhuang, Zou, Lei, Yang, & Zhao, 2012) but also possess effective bioactivities including antioxidant (Thetsrimuang, Khammuang, Chiablaem, Srisomsap, & Sarnthima, 2011), immunomodulatory (Hua et al., 2012), anti-tumor (Wu et al., 2011) and anti-inflammatory activates (Ovodova et al., 2009) etc. Recently, it has also been recognized that most polysaccharides are comparatively nontoxic and do not cause significant side effects. Thus, polysaccharides have attracted considerable interest from the food and pharmaceutical industries in developing nontoxic natural foods and food additives.

Schisandra sphenanthera Rehd. et Wits. is in the Magnoliaceae family and is widely distributed in the south-western and middle parts of China. The fruits of the species are commonly used as Traditional Chinese herbal medicines for liver and neural protection, treatment of cough and asthma, night sweating, palpitation and many other ailments (China's State Environmental Protection Administration). Current studies have demonstrated that *Schiasndra* are rich in different types of lignans (Liang et al., 2013), volatile oil and polysaccharides. However, most of these studies focused on the effect and structure of lignans (Chen et al., 2013; Huang et al., 2011; Liu et al., 2012; Song et al., 2013; Xiao et al., 2008) and there are few studies on polysaccharides in *Schisandra sphenanthera* Rehd. et Wits. In particular, the detailed structure elucidation and structure-activity correlation of the purified polysaccharide fraction have not been reported. Therefore, in this study, a polysaccharide fraction, SSPP11, was obtained by extraction and a DEAE-52 and Sephadex G-100 column. The structure of the SSPP11 was comprehensively analyzed by gas chromatography–mass spectrometry (GC–MS), 1D and 2D nuclear magnetic resonance (NMR) and the congo-red test. The antioxidant activity was also evaluated. This preliminary study focused on the correlation between the structure and antioxidant

* Corresponding author. Tel.: +86 511 88791800; fax: +86 511 88791800.
** Corresponding author. Tel.: +86 511 88791200; fax: +86 511 88791200.
E-mail addresses: yangliuqing@ujs.edu.cn (L. Yang), wuxy@ujs.edu.cn (X. Wu).

0144-8617/$ – see front matter © 2014 Elsevier Ltd. All rights reserved.
http://dx.doi.org/10.1016/j.carbpol.2014.01.059

activity. This information will be helpful in the recognition of biological systems for polysaccharides and the selection of active polysaccharides.

2. Materials and methods

2.1. Materials and reagents

The *Schisandra sphenanthera* Rehd. et Wits. was obtained from Zhenjiang Jiangyuan Co., Ltd., Zhengzhou, Henan province, China. DEAE-52 cellulose and Sephadex G-100 were purchased from Whatman Co., Ltd. Mw standards of T-series Dextran were obtained from Pharmacia Biotech (Uppsala, Sweden). Pure monosaccharide standards of D-mannose (Man), L-rhamnose (Rha), D-galactose (Gal), D-xylose (Xyl), D-arabinose (Ara), and D-glucose (Glu) were obtained from Sinopharm Chemical Reagent Co., Ltd. (Shanghai, China). 2,2-Diphenyl-2-picrylhydrazyl hydrate (DPPH) was obtained from Sigma–Aldrich. The other chemicals used were of reagent grade from commercial sources.

2.2. Isolation and purification of S. sphenanthera polysaccharide

A water-soluble polysaccharide was extracted from the fruits of *S. sphenanthera* according to our previous report (Zhao et al., 2013). Briefly, the powder of *S. sphenanthera* was pre-extracted for 12 h in a Soxhlet system with petroleum ether to remove lipids. After filtering, the residues were air dried at room temperature and extracted three times with boiling water in a ratio of 1:10 (w/v) for 3.0 h. After centrifugation, the supernatants were combined and were then concentrated using a rotary evaporator. The concentrated solution was mixed with five times the volume of 95% ethanol and kept at 4 °C for 24 h. The 15% trichloroacetic acid was added to the resulting precipitates slowly in an ice bath, until the pH reached 2–3 and kept 4 h at 4 °C for de-proteination, and then were dialyzed with dialysis bags with a molecular weight cut off of 3500 Da, which were then concentrated and freeze-dried to obtain the crude polysaccharide (SSP).

The 200 mg SSP was dissolved in distilled water and loaded onto a column (1.6 cm × 50 cm) of DEAE-52 cellulose. The column was sequentially eluted with 0, 0.05, 0.1, 0.15 and 0.2 M NaCl at a flow rate of 1 mL/min and each fraction of 6 mL of eluate was collected. The fractions were combined according to the carbohydrate content, as determined by the phenol-sulfuric acid method. Water eluates were further purified by a Sephadex G-100 column (1.6 cm × 50 cm). The column was eluted with 0.1 M NaCl at a flow rate of 0.3 mL/min, and the corresponding fractions were combined, dialyzed and freeze-dried, generating one water-soluble fraction (SSPP11).

2.3. Homogeneity and molecular weight determination

The homogeneity and molecular weight of SSPP11 were evaluated and determined by high performance liquid chromatography (HPLC, Shimadzu, Tokyo, Japan) on TSK-GEL G-4000PW columns (7.5 mm × 300 mm, Tosoh corporation, Tokyo, Japan) and were then eluted with a 0.003 mol/L CH_3COONa solution at a flow rate of 0.8 mL/min at 25 °C. The elution was monitored by a refractive index detector (Shimadzu RID-10A, Shimadzu). Different weight–average molecular weights of standard dextrans, T-2000, T-500, T-70, T-40 and T-10, were freshly prepared and injected into each run. The log [M_w] (Y) was regressed on the retention time (X) as $Y = -3.4754X + 6.5431$ ($R = 0.9991$).

2.4. Infrared spectrum analysis

The IR spectrum of SSPP11 was determined using a Fourier transform infrared spectrophotometer (NEXUS 670 FT-IR, Thermo Nicolet, USA). The purified polysaccharide was grounded with KBr powder and pressed into a 1 mm pellet for FTIR measurement between 400 and 4000 cm^{-1}.

2.5. Monosaccharide composition

SSPP11 (5 mg) was hydrolyzed with 2 M H_2SO_4 (2 mL) at 100 °C for 8 h in a sealed glass tube. After the neutralization of the residual H_2SO_4 with $BaCO_3$, ammonium hydrochloride and pyridine were added and allowed to react in a 90 °C water bath for 30 min. Next, 0.5 mL of acetic anhydride was added to the test tube, and the mixture was incubated at 90 °C for a further 30 min to allow the acetylation reaction to occur. The acetylated derivatives were analyzed by GC with a HP-5MS column (0.25 mm × 30 m × 0.25 μm) and a flame-ionization detector. The temperature programme was set at 130 °C and maintained for 5 min and was then increased to 240 °C at an increment of 5 °C/min, the 240 °C temperature was held for 5 min. Standard monosaccharides were measured following the same procedure.

2.6. Methylation analysis

Methylation analysis was carried out according to the method of Needs and Selvendran (1993) (Han et al., 2011; Needs & Selvendran, 1993; Pan et al., 2012; Scoparo et al., 2013). Briefly, 5 mg of SSPP11 were dissolved in 2 mL of anhydrous dimethylsulfoxide (DMSO) in a three-necked flask at room temperature (25 °C) with a nitrogen inlet. Then, 100 mg of NaOH was added, and the mixture was stirred for 1 h at room temperature (25 °C) with a nitrogen inlet. Methyl iodide (1 mL) was added and maintained for 4 h at room temperature (25 °C). The product was then extracted five times with 2 mL of dichloromethane. The dichloromethane layer was washed five times with 2 mL of distilled water, and the dichloromethane was then dried at room temperature. The residues were depolymerized with 85% formic acid at 100 °C for 6 h and further hydrolyzed with 2 M trifluoroacetic acid at 100 °C for 6 h in a sealed tube. Excess trifluoroacetic acid was removed by evaporation under reduced pressure. Next, 25 mg of $NaBH_4$ was added to reduce the uronic acid and 0.1 mL of glacial acetic acid was added after the reduction. The residue was dissolved in methanol and evaporated to dryness three times. The partially methylated residues were acetylated by 0.5 mL of acetic anhydride and 0.5 mL of pyridine at 100 °C for 1 h. The resulting partially methylated alditol acetates (PMAA) were extracted with methylene chloride and analyzed with a GC–MS (6890 N/5975B GC-MS, Agilent, USA), which equipped with a HP-5 column (0.25 mm × 30 m × 0.25 μm). The temperature was set as follows: initial temperature of the column was 130 °C, maintained at 130 °C for 5 min and then the temperature was increased to 240 °C at 4 °C/min. The 240 °C temperature was held for 5 min. PMAA were identified by their fragment ions in according to the MS spectrum and the relative retention time on GC profile.

2.7. NMR analysis

20 mg of SSPP11 sample was deuterium-exchanged in D_2O, freeze-dried and redissolved in 0.5 mL of D_2O. Then, 1D ^1H NMR (400 MHz), ^{13}C NMR (100 MHz), and 2D NMR spectra of SSPP11 were recorded on a Bruker DRX-400 spectrometer (Bruker, Rheinstetten, Germany) at 296.9 K. The scans number in the ^{13}C NMR spectra was 25,000. The chemical shift was expressed in ppm.

2.8. Helix-coil transition assay

The conformational structure of the polysaccharides in solution was determined using characterizing Congo red-polysaccharide complexes. The transition from a triple-helical arrangement to the single-stranded conformation was examined by measuring the λ_{max} of the Congo red-polysaccharide solutions at different NaOH concentrations that ranged from 0 to 0.5 M. The polysaccharide samples (5 mg) were dissolved in 2 mL of distilled water and were mixed with 80 μM Congo red solution (2 mL). Drops of a 1 M NaOH solution were added to a mixed solution to achieve a final concentration of NaOH in the mixed solution being 0.0 M, 0.1 M, 0.15 M, 0.2 M, 0.25 M, 0.3 M, 0.35 M, 0.4 M, 0.45 M and 0.5 M, respectively. The UV–visible spectra of the mixture at various NaOH concentrations were scanned with a UV-visible spectrophotometer (TU-1800, China) at 400–800 nm and the maximum absorption wavelength was recorded. In another reaction system, distilled water, instead of a polysaccharides solution, was mixed with a Congo red and NaOH solution. The visible spectra were also scanned using the same method that was used for the SSPP11 mixed with the Congo red and NaOH solution (Liu et al., 2011; Yu et al., 2010).

2.9. Antioxidant activities

The DPPH free radical scavenging activity of each sample was determined according to the method described by D. Qiao (Qiao et al., 2009; You, Yin, Zhang, & Jiang, 2014) with some modifications. 2.0 mL DPPH·solution (2×10^{-4} mol/L in dehydrated alcohol) was added to different concentrations of polysaccharide solution (2.0 mL). The mixture was shaken and allowed to settle for 30 min in the dark. In this assay, ascorbic acid was used as a standard antioxidant to validate the assay. The DPPH radical scavenging effect was determined using the following equation: Scavenging rate = $[1 - (A_i - A_j)/A_0] \times 100\%$.

3. Results and discussion

3.1. Extraction and purification of crude polysaccharide

The crude polysaccharide was isolated from the hot water extract of *S. sphenanthera* with a yield of 12.91%. After fractionation on a DEAE-52 column, five fractions were obtained. The Sephadex G-100 column was then used for further purification and the distilled water eluent, SSPP11, was obtained. The gel filtration chromatograms of the SSPP11 are shown in Fig. 1A and reveal that the fraction was represented by a single and symmetrical peak which indicates the high purity of the generated SSPP11.

3.2. Basic properties of SSPP11

High-performance gel permeation chromatography (HPGPC) was applied to determine the molecular weights of SSPP11 by using the dextran standards and the HPGPC chromatograms of SSPP11 are shown in Fig. 1B. The equivalent dextran molecular weights of SSPP11 were approximately 5.3×10^3 Da, which was higher than that of a polysaccharide fraction from *Schisandra chinensis* (Turcz.) Baill (named SCPP11) (Zhao et al., 2013).

The monosaccharide composition of the SSPP11 fraction that was analyzed by GC, is shown in Fig. 1C. The peaks of all of the monosaccharides were sharp and symmetrical. Compared with the monosaccharide standards (Zhao et al., 2013), the peaks of the SSPP11 fraction were identified as D-mannose, D-glucose and D-galactose, with molar ratios of 1:1.77:1.29, which indicated that the SSPP11 was heterogeneous. The results also indicated that D-glucose was the major monosaccharide component of the backbones of SSPP11. In our previous study, the monosaccharide composition of SCPP11 was identical to SSPP11, but it showed a much higher molar ratio of D-glucose (71%) (Zhao et al., 2013).

The IR spectra of SSPP11 are shown in Fig. 1D. The characteristic strong broad band of approximately 3404 cm^{-1} was attributed to the hydroxyl stretching vibration of the polysaccharides. The weak bands at 2924 cm^{-1} were due to the C—H stretching vibration in carbohydrates, and the band at 1373 cm^{-1} was assigned to C—H bending vibration. The band at 1636 cm^{-1} was due to the presence of bound water. The peaks in the range of 1044–1150 cm^{-1} were attributed to the stretching vibration of C—O—C group. The absorption peak at 350–660 cm^{-1} indicated that this was a pyran-type polysaccharide.

3.3. Linkage features of SSPP11

To determine the linkages of the monosaccharides in SSPP11, SSPP11 was methylated, depolymerized, hydrolyzed and acetylated for a GC–MS analysis. The peaks of methylated sugars were identified according to their retention times and mass spectra. The GC chromatogram and the linkage patterns of SSPP11 are shown in Fig. 2A and Table 1. The results indicated that SSPP11 had ten different glycosidic linkages, and these molar ratios agreed with the overall monosaccharide composition described above. It was shown that SSPP11 was composed mainly of T-D-Man*p*(1→, →1)-D-Man-(6→, T-D-Glu*p*(1→, T-D-Gal*p*(1→, →1)-D-Man*p*-(2→, →1)-D-Glu*p*(4→, →1)-D-Glu*p*-(6→, →1)-D-Gal*p*-(4→, →1)-D-Gal*p*-(4,6→ and →1)-D-Man*p*-(3,6→ in a 1.1:4.8:6.2:5.2:4.8:15.4:21.6:20.8:1:11.4 ratio. In addition, the presence of →1)-D-Gal*p*-(4,6→ and →1)-D-Manp-(3,6→ showed that there is a relatively high degree of branching in the SSPP11 polysaccharide, which was notably different from the SCPP11 polysaccharide. The ratio between the apparent terminal units and branching point is 1.01, which is consistent with the fact that the number of polysaccharide branching points approximately equal the number of terminal units.

3.4. Determination of the sugar residues and their sequence by NMR

The ^1H and ^{13}C NMR, COSY, HSQC and HMBC NMR are shown in Fig. 2. The completely assigned spectrum of SSPP11 is given in Table 2, which was derived from the 1D and 2D NMR spectra.

The ^1H NMR spectrum of SCPP11 is shown in Fig. 2(B). The signals at 5.0–5.4 and 4.4–5.0 ppm were assigned as the anomeric protons of the α-glycosidical configuration and β-glycosidical configuration. The ^1H NMR spectrum of SSPP11 showed ten anomeric proton signals at δ 5.18, 5.13, 5.05, 4.93, 4.86, 4.56, 4.54, 4.50, 4.45 and 4.45 ppm. The sugar residues were assigned as A, I, D, E, C, G, H, B, F and J. The three low-field signals represent sugars with an α-anomeric configuration and the other high-field signals represent sugars with a β-anomeric configuration. The ^{13}C NMR spectrum (Fig. 2(C)) contained signals for ten anomeric carbons at 104.44–96.28 ppm.

Residue A had been confirmed to be an α-glycosidical residue. The COSY spectrum showed stepwise connectivities from the H-1 signal at 5.18 ppm to H-2 at 3.59 ppm, H-3 signal at 3.64 ppm, H-4 signal at 3.871 ppm, H-5 signal at 4.08 ppm and H-6 signal at 3.55 ppm. The HMBC spectrum (Fig. 2(F)) showed correlations between C-4 at δ 69.99 ppm and H-3, H-5 and H-6 signals at δ 3.64 ppm, 4.08 ppm and 3.46 ppm, respectively. After the protons were identified, the chemical shifts of their corresponding carbons were determined from the HSQC spectrum between the carbon and proton in C-H pairs. The carbon signals from C-1 to C-6 were identified according to $^1H/^{13}C$ heteronuclear single quantum correlation (HMQC) spectroscopy (Fig. 2(E)). The downfield shift of C-1 with respect to the standard value, and no carbon signal was evident

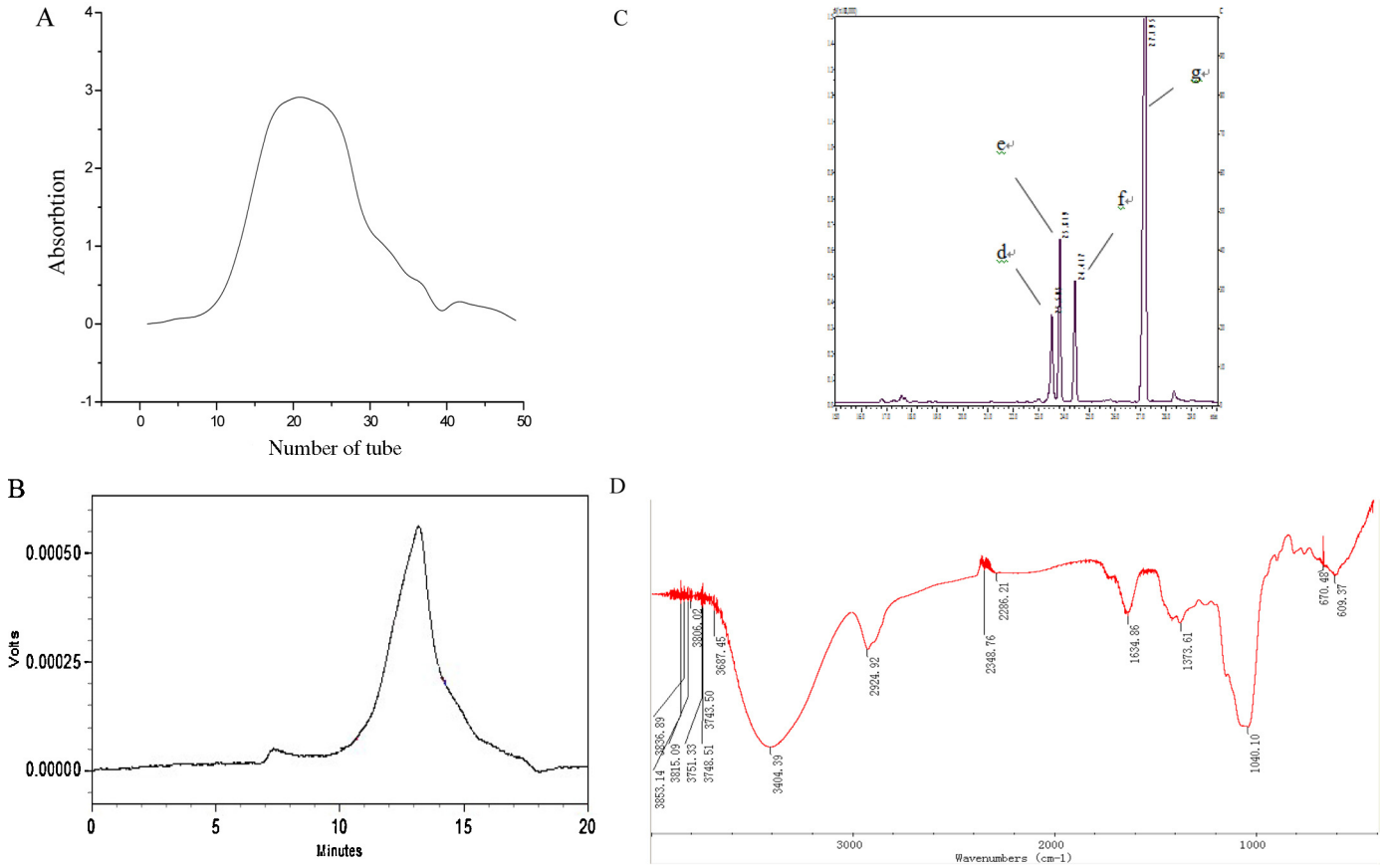

Fig. 1. (A) One fraction purified by Sephadex G-100, SSPP11. (B) HPGPC elution profiles of the SSPP11 with refractive index detector. (C) Gas chromatograms of the monosaccharide compositions of the SSPP11. (D) FT-IR spectrum of SSPP11 from *Schisandra sphenanthera* Rehd. et Wits.

in the δ 76–82, indicating that residue A was substituted at C-1. Residue A was identified as a 1-substituted α-D mannopyranose.

Residue B had an anomeric chemical shift at δ 4.50. Using similar approaches, the COSY spectrum showed connectivities from the H-1 signal at δ 4.50 ppm to the H-2 signal at δ 3.40 ppm and the H-3 signal at δ 3.50 ppm, from the H-3 signal to the H-4 signal at δ 3.75 ppm and the H-5 signal at δ 4.05 ppm, and from the H-5 signal to the H-6 signal at δ 3.71 ppm. On the basis of the proton assignments, the corresponding ^{13}C chemical shifts were readily assigned from the HSQC spectrum (Fig. 2(E)) between the carbons and protons of the C-H pairs (Table 2). The HMBC spectrum demonstrated correlations between δ 70.11 ppm (C-3) with δ 3.40 ppm (H-2), and 3.75 ppm (H-4). The downfield shifts of the C-1 (δ 96.28 ppm) and C-6 (δ 69.99 ppm) carbon signals confirmed that residue B was a 1,6-disubstituted β-D-mannopyranose.

The proton and carbon chemical shifts of residue C, beginning from the peak at 4.86 ppm (H-1), were obtained using the above approaches. The 1H chemical shifts from the H-1 signal at 4.86 to the H-2 signal at 3.61 and to the H-3 signal at 3.67 were assigned. The assignments of H-4, H-5 and H-6 were determined by cross peaks in the HMBC spectrum, including correlations between C-3 (71.82) and H-4 (3.81) and H-5 (4.08) as well as C-4 (70.09) and H-6 (3.51). Their corresponding ^{13}C chemical shifts were assigned, based on the C-H pairs in the HSQC spectrum. The downfield shift of C-1, with reference respect to the standard value and no carbon signal, was evident in the δ 76–82, indicating that residue C was substituted at C-1. Residue C was identified as a 1-substituted α-D glucopyranose.

Using similar approaches, residue D, E, F, G, H, I and J had an anomeric proton signal at δ 5.05, 4.93, 4.51, 4.56, 4.54, 5.13, 4.45 ppm, respectively. The H signals in the ^{1}H NMR spectra were assigned according to COSY combined with HSQC and HMBC. Their corresponding ^{13}C chemical shifts were readily assigned from the HSQC spectrum between the carbons and protons of the C-H

Table 1
Linkage analysis of the SSPP11 isolated from *Schisandra sphenanthera* Rehd. et Wits.

Number	Retention time (min)	PMAA	Linkage pattern	Ion fragmentation	Peak area percentage(%)	Molar ratio
A	5.19	2,3,4,6-Me$_4$-Man*p*	T-Man*p*	43, 71, 87, 101, 117, 129, 145, 161, 205	1.20	1.11
B	5.97	2,3,4-Me$_3$-Man*p*	1,6-linked-Gal*p*	43, 58, 71, 87, 101, 117, 129, 161, 189, 233	5.53	5.12
C	6.19	2,3,4,6-Me$_4$-Glu*p*	T-Glu*p*	43, 59, 71, 87, 101, 117, 145, 161, 205	6.68	6.19
D	6.48	2,3,4,6-Me$_4$-Gal*p*	T-Gal*p*	43, 59, 71, 87, 101, 117, 129, 145, 161, 205	5.64	5.22
E	7.24	3,4,6-Me$_3$-Man*p*	1,2-linked-Man*p*	43, 59, 71, 87, 101, 129, 145, 161, 189, 233	5.2	4.81
F	7.46	2,3,6-Me$_3$-Glu*p*	1,4-linked-Glu*p*	43, 71, 101, 117, 129, 161, 233	16.67	15.44
G	7.54	2,3,4-Me$_3$-Man*p*	1,6-linked-Glu*p*	43, 71, 101, 117, 129, 161, 189, 233	23.35	21.62
H	7.69	2,3,6-Me$_3$-Gal*p*	1,4-linked-Gal*p*	43, 71, 101, 117, 129, 161, 189, 233	22.41	20.75
I	9.12	2,3-Me$_2$-Gal*p*	1,4,6-linked-Gal*p*	43, 87, 99, 101, 117, 129, 161, 189	1.08	1
J	9.22	2,4-Me$_2$-Man*p*	1,3,6-linked-Man*p*	43, 87, 99, 118, 129, 189, 233	12.10	11.20

Table 2
Chemical shift (δ) assignments of ^{1}H NMR and ^{13}C NMR spectra of SSPP11 on the basis of COSY, HSQC and HMBC.

Residues		The chemical shift of ^{1}H and ^{13}C (ppm)					
		1	2	3	4	5	6
(A) α-D-Man *p*-(1→	H	5.18	3.59	3.64	3.87	4.08	3.46
	C	99.99	77.92	72.63	69.98	70.55	61.87
(B) →1)-β-D-Man*p*-(6→	H	4.96	3.39	3.50	3.75	4.06	3.66
	C	96.28	69.83	70.11	68.26	70.22	69.99
(C) β-D-Glu*p*-(1→	H	4.86	3.61	3.67	3.814	4.08	3.51
	C	98.92	70.01	71.82	70.09	70.58	62.02
(D) α-D-Gal*p*-(1→	H	5.10	3.44	3.57	3.79	4.08	3.59
	C	98.76	72.06	72.77	73.94	71.92	63.79
(E) →1)-β-D-Man*p*-(2→	H	4.93	3.65	3.71	3.90	4.13	3.55
	C	98.92	73.65	69.57	68.27	69.18	60.93
(F) →1)-β-D-Glu*p*-(4→	H	4.45	3.29	3.59	4.09	4.03	3.48
	C	104.36	70.08	72.06	77.65	72.06	63.50
(G) →1)-β-D-Glu*p*-(6→	H	4.56	3.57	3.61	3.72	4.02	3.61
	C	104.44	69.59	70.00	69.98	70.55	68.63
(H) →1)-β-D-GAL*p*-(4→	H	4.54	3.27	3.51	4.08	4.09	3.51
	C	102.69	69.98	71.48	78.30	70.88	63.53
(I) →1)-α-D-Gal*p*-(4,6→	H	5.13	3.64	3.72	4.08	4.16	3.65
	C	99.99	70.68	72.77	77.65	70.57	67.76
(J) →1)-β-D-Man*p*-(3,6→	H	4.45	3.43	3.85	3.87	4.19	3.65
	C	104.36	69.23	78.23	72.06	70.57	69.47

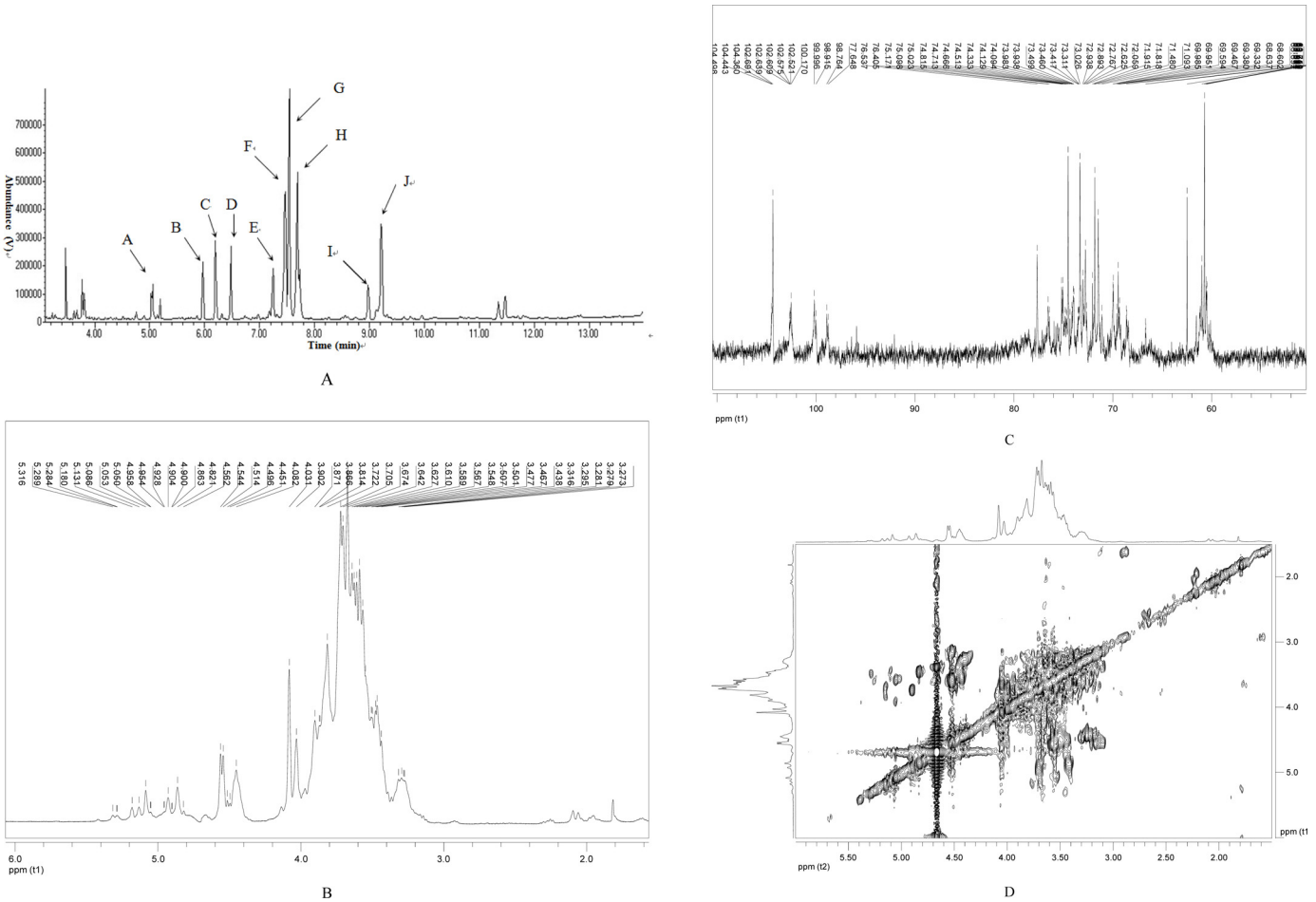

Fig. 2. (A) The total ion chromatogram from methylation analysis of SSPP11 fraction. (B) The ^{1}H NMR spectra of SCPP11. (C) The ^{13}C NMR spectra of SCPP11. (D) ^{1}H/^{1}H COSY correlation spectra of SSPP11. (E) ^{1}H/^{13}C HSQC correlation spectra of SSPP11. (F) ^{1}H/^{13}C HMBC correlation spectra of SSPP11. (G) Chemical structure of polysaccharide SSPP11.

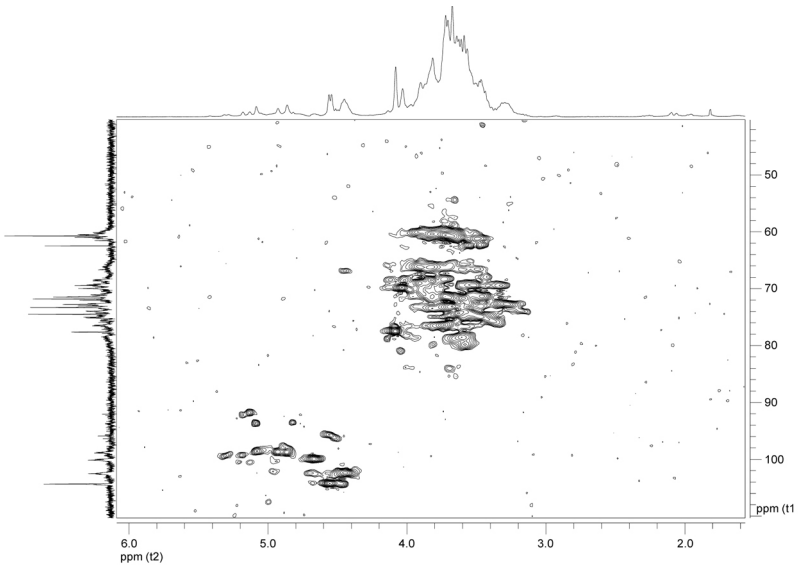

E

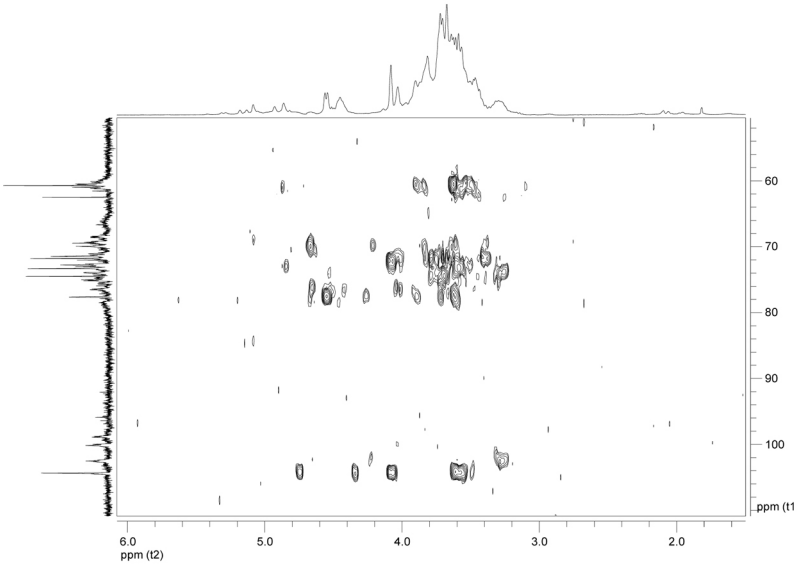

F

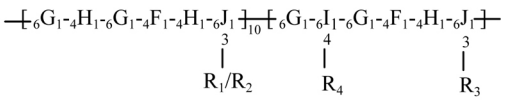

$R_1 : R_2 : R_3 : R_4 = 5 : 5 : 1 : 1$

R_1 : $_1E_2$-$_1C$

R_2 : $_1B_6$-$_1D$

R_3 : $_1F_4$-$_1F_4$-$_1C$

R_4 : $_1F_4$-$_1F_4$-$_1A$

G

Fig. 2. (*Continued*)

pairs. In addition, the downfield shifts of C-1, C-1 and C-2; C-1 and C-4; C-1 and C-6; C-1 and C-4; C-1, C-4 and C-6; and C-1, C-3 and C-6 carbon signals also indicated that residue D, E, F, G, H, I and J were 1-substituted α-D galactopyranose, 1,2-disubstituted β-D-mannopyranose, 1,4-disubstituted β-D-glucopyranose, 1,6-disubstituted β-D-glucopyranose, 1,6-disubstituted β-D-galactopyranose, 1,4-disubstituted β-D-galactopyranose, 1.4,6-trisubstituted β-D-galactopyranose and 1,3,6-disubstituted β-D-mannopyranose, respectively.

Long-range ^{13}C–^{1}H correlations obtained from the HMBC spectrum (Fig. 2(F)) confirmed the glycosyl sequence of SSPP11. The cross-peaks of both the anomeric protons and carbons of each residue were examined, and intra- and inter-residual connectivities were observed from the HMBC experiment. Cross-peaks were found between A H-1 and F C-4 indicating that residue A was linked at the 4-position of residue F. Residue B and Residue E had inter-residue correlations from C-1 to H-3 of residue J, respectively, indicating that residue B and residue E were linked at the 3-position of residue J. The inter-residue correlations were observed between C C-1 and E H-2, which were indicative of C (1→2)E linkages. Residue D had inter-residue correlations from the H-1 to C-6 of residue B, indicating that residue D linked at the 6-position of residue B. Moreover, the HMBC spectrum demonstrated inter-residue correlations between F C-1 and F H-4 and between F C-1 and I H-4, between F C-1 and H H-4, and between F H-1 and J C-3, which are indicative of F (1→4)F, F (1→4)I, F (1→4)H and F (1→3)J linkages. In addition, the inter-residue correlations between G C-1 and H H-4, G C-1 and F H-4, G C-1 and I H-6, H C-1 and G H-6, H C-1 and J H-6 and J C-1 and G H-6 were an indication of G(1→4)H, G(1→4)F, G(1→6)I, H(1→6)G, H(1→6)J and J(1→6)G linkages. The results indicated that SSPP11 possess more side chains than SCPP11.

Therefore, based on the chemical and spectroscopic findings, the predicted primary structure of the SSPP11 was established and is shown in Fig. 2(G).

3.5. Helix-coil transition assay

The presence of polysaccharides induced a shift in the visible absorption maximum of Congo red, which is a rapid method for detecting conformational information. Generally, if the wavelength

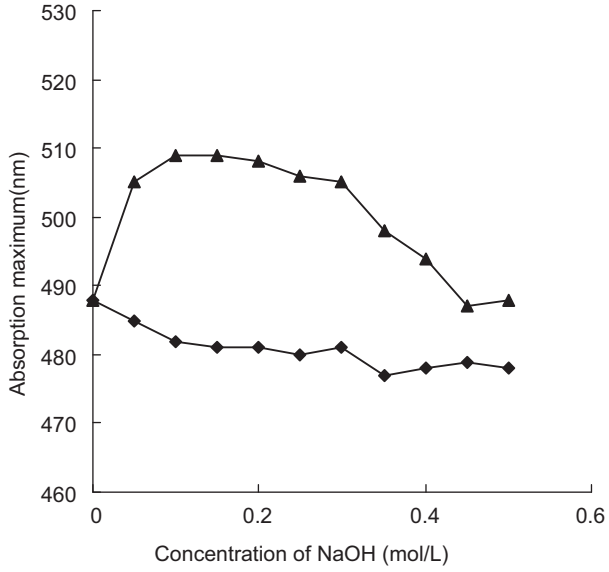

Fig. 3. Helix-coil transition analysis of SSPP11 according to the absorption maximum of the congo red-polysaccharide complex at various concentrations of NaOH.

of the maximum absorption of the complex with Congo red shifts to beyond 505 nm in 0.1 M sodium hydroxide, it is concluded that the polysaccharide possesses a triple-helical structure in an aqueous solution. The λ_{max} of the SSPP11-Congo red complexes at a NaOH concentration range of 0–0.5 M is shown in Fig. 3. It is evident that at low concentrations (0–0.10 M), the λ_{max} shifted to a longer wavelength, 509 nm for SSPP11. When the concentration of NaOH was increased by more than 0.20 M, the λ_{max} slowly dropped. This indicated that SSPP11 most likely adopted a highly ordered conformation, which remained stable even under strong alkaline conditions (Vasconcelos et al., 2008).

3.6. Antioxidant activity

The model of scavenging the DPPH radical is a widely used method for evaluating the free radical-scavenging ability of polysaccharide (Chen, Xie, Nie, Li, & Wang, 2008; Qiao et al., 2009). The antioxidant mechanism of DPPH radical scavenging is based on the acceptance of hydrogen by the DPPH radical, thereby converting DPPH into the non-radical form (DPPH-H). Thus the antioxidant activity is due to the hydrogen-donating ability of the polysaccharide (Yang et al., 2011). The —OH groups in the polysaccharide play an important role in its antioxidant activity. Fig. 4 shows the DPPH radical scavenging activity of SSPP11. The results indicated that SSPP11 showed dose-dependent DPPH radical scavenging activities in all of the evaluated concentrations. At a concentration of 1500 μg/mL, the DPPH radical scavenging activity was 45%, which was nearly twice as much as SCPP11 (22%).

3.7. Structure–activity correlation

The molecular weights of polysaccharides play an important role in their bioactivity. Recent studies have suggested that the moderate molecular weights are beneficial to polysaccharides for exerting their activities (Liu, Wang, Pang, Yao, & Gao, 2010; Sun, Wang, Shi, & Ma, 2009; Zou, Du, Li, Yang, & Zhang, 2010). In our study, polysaccharides of 5.3 kDa (SSPP11) exhibited stronger antioxidant activity than those of 3.4 kDa. Moreover, the antioxidant activity of polysaccharides is usually not a function of one single factor but rather a combination of factors. The SSPP11 possesses more side chains and it is more beneficial for the exposure of

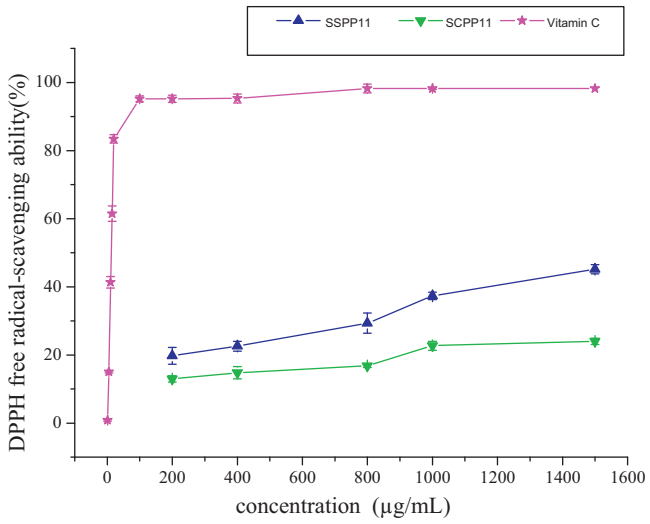

Fig. 4. Antioxidant activities of SSPP11 in DPPH free radical-scavenging assays.

—OH groups in SSPP11, which is different with SCPP11. In conclusion, the moderate molecular weights, configuration and degree of branching maybe related to SSPP11 antioxidant activity.

4. Conclusions

In this study, polysaccharides were obtained from *S. sphenanthera* using a DEAE-52 and Sephadex G-100 column. SSPP11's molecular weight was approximately 5.3 kDa, and it was composed of D-mannose, D-glucose and D-galactose with molar ratios of 1:1.77:1.29. The structural study demonstrated that SSPP11 had a backbone of →1)-D-Glu*p*(4→, →1)-D-Glu*p*-(6→, →1)-D-Gal*p*-(4→, and with branch at the C-3 position of 1)-D-Man*p*-(6→. SSPP11 was also confirmed to have a triple helix stereo-configuration. Moreover, the SSPP11 exhibited a stronger capacity than SCPP11 for scavenging the DPPH free radical, which may be related to its moderate molecular weight, configuration and degree of branching. It is therefore recommended that SSPP11 could be explored as a potential novel antioxidant. The chemical structural modification and further structure–activity relationships would be investigated in the future.

Acknowledgment

This work was supported financially by Natural Science Fund of Jiangsu Province (BK2012702). We also appreciate Dr. Mohammed Takase and Dr. Samuel Jerry Cobbina for language polishing.

References

Chen, Y.-C., Liaw, C.-C., Cheng, Y.-B., Lin, Y.-C., Chen, C.-H., Huang, Y.-T., Liou, S.-S., Chen, S.-Y., Chien, C.-T., Lee, G.-C., & Shen, Y.-C. (2013). Anti-liver fibrotic lignans from the fruits of *Schisandra arisanensis* and *Schisandra sphenanthera*. *Bioorganic & Medicinal Chemistry Letters*, *23*(3), 880–885.

Chen, Y., Xie, M.-Y., Nie, S.-P., Li, C., & Wang, Y.-X. (2008). Purification, composition analysis and antioxidant activity of a polysaccharide from the fruiting bodies of *Ganoderma atrum*. *Food Chemistry*, *107*(1), 231–241.

Han, X.-Q., Wu, X.-M., Chai, X.-Y., Chen, D., Dai, H., Dong, H.-L., Ma, Z.-Z., Gao, X.-M., & Tu, P.-F. (2011). Isolation, characterization and immunological activity of a polysaccharide from the fruit bodies of an edible mushroom, *Sarcodon aspratus* (Berk.) S. Ito. *Food Research International*, *44*(1), 489–493.

Hua, Y. L., Gao, Q., Wen, L. R., Yang, B., Tang, J., You, L. J., & Zhao, M. M. (2012). Structural characterisation of acid- and alkali-soluble polysaccharides in the fruiting body of *Dictyophora indusiata* and their immunomodulatory activities. *Food Chemistry*, *132*(2), 739–743.

Huang, H. C., Lin, Y. C., Fazary, A. E., Lo, I. W., Liaw, C. C., Huang, Y. Z., Liou, S. S., & Shen, Y. C. (2011). New and bioactive lignans from the fruits of *Schisandra sphenanthera*. *Food Chemistry*, *128*(2), 348–357.

Liang, C. Q., Hu, J., Luo, R. H., Shi, Y. M., Shang, S. Z., Gao, Z. H., Wang, R. R., Zheng, Y. T., Xiong, W. Y., Zhang, H. B., Xiao, W. L., & Sun, H. D. (2013). Six new lignans from the leaves and stems of *Schisandra sphenanthera*. *Fitoterapia*, *86*(0), 171–177.

Lin, L. Z., Zhuang, M. Z., Zou, L. W., Lei, F. F., Yang, B., & Zhao, M. M. (2012). Structural characteristics of water-soluble polysaccharides from Rabdosia serra (MAXIM.) HARA leaf and stem and their antioxidant capacities. *Food Chemistry*, *135*(2), 730–737.

Liu, H. T., Zhang, J., Li, X. B., Qi, Y. D., Peng, Y., Zhang, B. G., & Xiao, P. G. (2012). Chemical analysis of twelve lignans in the fruit of *Schisandra sphenanthera* by HPLC–PAD-MS. *Phytomedicine*, *19*(13), 1234–1241.

Liu, J. C., Zhang, C. H., Wang, Y. J., Yu, H. T., Liu, H., Wang, L. P., Yang, X. Z., Liu, Z. C., Wen, X. C., Sun, Y. X., Yu, C. L., & Liu, L. (2011). Structural elucidation of a heteroglycan from the fruiting bodies of *Agaricus blazei* Murill. *International Journal of Biological Macromolecules*, *49*(4), 716–720.

Liu, W., Wang, H. Y., Pang, X. B., Yao, W. B., & Gao, X. D. (2010). Characterization and antioxidant activity of two low-molecular-weight polysaccharides purified from the fruiting bodies of *Ganoderma lucidum*. *International Journal of Biological Macromolecules*, *46*(4), 451–457.

Mao, G. H., Zou, Y., Feng, W. W., Wang, W., Zhao, T., Ye, C. W., Zhu, Y., Wu, X. S., Yang, L. Q., & Wu, X. Y. (2014). Extraction, preliminary characterization and antioxidant activity of Se-enriched Maitake polysaccharide. *Carbohydrate Polymers*, *101*(0), 213–219.

Needs, P. W., & Selvendran, R. R. (1993). Avoiding oxidative degradation during sodium hydroxide/methyl iodide-mediated carbohydrate methylation in dimethyl sulfoxide. *Carbohydrate Research*, *245*(1), 1–10.

Ovodova, R. G., Golovchenko, V. V., Popov, S. V., Popova, G. Y., Paderin, N. M., Shashkov, A. S., & Ovodov, Y. S. (2009). Chemical composition and anti-inflammatory activity of pectic polysaccharide isolated from celery stalks. *Food Chemistry*, *114*(2), 610–615.

Pan, D., Wang, L., Chen, C., Teng, B., Wang, C., Xu, Z., Hu, B., & Zhou, P. (2012). Structure characterization of a novel neutral polysaccharide isolated from *Ganoderma lucidum* fruiting bodies. *Food Chemistry*, *135*(3), 1097–1103.

Qiao, D. L., Ke, C. L., Hu, B., Luo, J. G., Ye, H., Sun, Y., Yan, X. Y., & Zeng, X. X. (2009). Antioxidant activities of polysaccharides from *Hyriopsis cumingii*. *Carbohydrate Polymers*, *78*(2), 199–204.

Scoparo, C. T., de Souza, L. M., Rattmann, Y. D., Dartora, N., Paiva, S. M. M., Sassaki, G. L., Gorin, P. A. J., & Iacomini, M. (2013). Polysaccharides from green and black teas and their protective effect against murine sepsis. *Food Research International*, *53*(2), 780–785.

Song, Q. Y., Zhang, C. J., Li, Y., Wen, J., Zhao, X. W., Liu, Z. L., & Gao, K. (2013). Lignans from the fruit of *Schisandra sphenanthera*, and their inhibition of HSV-2 and adenovirus. *Phytochemistry Letters*, *6*(2), 174–178.

Sun, L., Wang, C., Shi, Q., & Ma, C. (2009). Preparation of different molecular weight polysaccharides from *Porphyridium cruentum* and their antioxidant activities. *International Journal of Biological Macromolecules*, *45*(1), 42–47.

Thetsrimuang, C., Khammuang, S., Chiablaem, K., Srisomsap, C., & Sarnthima, R. (2011). Antioxidant properties and cytotoxicity of crude polysaccharides from *Lentinus polychrous* Lév. *Food Chemistry*, *128*(3), 634–639.

Vasconcelos, A. F. D., Monteiro, N. K., Dekker, R. F. H., Barbosa, A. M., Carbonero, E. R., Silveira, J. L. M., Sassaki, G. L., da Silva, R., & de Lourdes Corradi da Silva, M. (2008). Three exopolysaccharides of the β-(1→6)-d-glucan type and a β-(1→3;1→6)-d-glucan produced by strains of *Botryosphaeria rhodina* isolated from rotting tropical fruit. *Carbohydrate Research*, *343*(14), 2481–2485.

Wang, M. C., Jiang, C. X., Ma, L. P., Zhang, Z. J., Cao, L., Liu, J., & Zeng, X. X. (2013). Preparation, preliminary characterization and immunostimulatory activity of polysaccharide fractions from the peduncles of *Hovenia dulcis*. *Food Chemistry*, *138*(1), 41–47.

Wu, X. Y., Mao, G. H., Fan, Q. Y., Zhao, T., Zhao, J. L., Li, F., & Yang, L. Q. (2012). Isolation, purification, immunological and anti-tumor activities of polysaccharides from *Gymnema sylvestre*. *Food Research International*, *48*(2), 935–939.

Wu, X. Y., Mao, G. H., Zhao, T., Zhao, J. L., Li, F., Liang, L. H., & Yang, L. Q. (2011). Isolation, purification and in vitro anti-tumor activity of polysaccharide from Ginkgo biloba sarcotesta. *Carbohydrate Polymers*, *86*(2), 1073–1076.

Xiao, W. L., Huang, S. X., Wang, R. R., Zhong, J. L., Gao, X. M., He, F., Pu, J. X., Lu, Y., Zheng, Y. T., Zheng, Q. T., & Sun, H. D. (2008). Nortriterpenoids and lignans from *Schisandra sphenanthera*. *Phytochemistry*, *69*(16), 2862–2866.

You, Q. H., Yin, X. L., Zhang, S. N., & Jiang, Z. H. (2014). Extraction, purification, and antioxidant activities of polysaccharides from *Tricholoma mongolicum* Imai. *Carbohydrate Polymers*, *99*, 1–10.

Yu, Z., Ming, G., Kaiping, W., Zhixiang, C., Liquan, D., Jingyu, L., & Fang, Z. (2010). Structure, chain conformation and antitumor activity of a novel polysaccharide from Lentinus edodes. *Fitoterapia*, *81*(8), 1163–1170.

Zhao, T., Mao, G. H., Mao, R. W., Zou, Y., Zheng, D. H., Feng, W. W., Ren, Y. N., Wang, W., Zheng, W., Song, J., Chen, Y. Q., Yang, L. Q., & Wu, X. Y. (2013). Antitumor and immunomodulatory activity of a water-soluble low molecular weight polysaccharide from *Schisandra chinensis* (Turcz.) Baill. *Food and Chemical Toxicology*, *55*, 609–616.

Zhu, Y., Li, Q., Mao, G. H., Zou, Y., Feng, W. W., Zheng, D. H., Wang, W., Zhou, L. L., Zhang, T. X., Yang, J., Yang, L. Q., & Wu, X. Y. (2014). Optimization of enzyme-assisted extraction and characterization of polysaccharides from *Hericium erinaceus*. *Carbohydrate Polymers*, *101*, 606–613.

Zou, C., Du, Y., Li, Y., Yang, J., & Zhang, L. (2010). Preparation and in vitro antioxidant activity of lacquer polysaccharides with low molecular weights and their sulfated derivatives. *International Journal of Biological Macromolecules*, *46*(2), 140–144.